JOURNAL OF OPTOELECTRONICS AND ADVANCED MATERIALS Vol. 16, No. 1 - 2, January – February 2014, p. 47- 51

Design of a new single star simulator for multi-colour temperature and wide-magnitude-range output

LU DONG[a], TAO ZHANG[a,*], LI HOU[a], YANHUA WU[b]
[a]*School of Manufacturing Science and Engineering, Sichuan University, Chengdu 610065, P. R. China*
[b]*State Key Laboratory of Hydraulics and Mountain River Engineering , Sichuan University, Chengdu 610065, P. R. China*

To overcome the shortcomings of traditional single star simulators, a new single star simulator is designed to achieve multi-colour temperature and wide-magnitude-range output. Its colour temperature and magnitude do not affect each other and can be adjusted in real time. The basic principle is to mix a number of light rays of different narrow-band spectrums and intensities to control the whole intensity. The system's overall structure, including the structure of the light source, the band intensity controller and the magnitude controller was designed. The assembly and testing were completed. The results show that the system can simulate numerous colour temperatures with a relative error less than ±0.10 and a simulated magnitude range of 0~+6.5 MI with an error less than ±0.3 MI. This flexibly operated system is stable and reliable. This research has already been used in related equipment with positive operational results, which serves as a reference for further studies.

(Received October 20, 2013; accepted January 22, 2014)

Keywords: Star simulator, Colour temperature, Magnitude, Spectrum, Light intensity

1. Introduction

With the in-depth development of aerospace technology, star sensors have been widely used for measuring the position and attitude of aerospace equipment in space inertial coordinate systems [1-3]. Thus, the calibration technology requirements for star sensors are becoming increasingly more rigorous.

The single star simulator is one of the main ground calibration components of star sensors. Its primary task is to simulate the stellar light source with photometric, spectral and geometric properties similar to a real star. The properties of the star simulator directly influence the measurement accuracy of the star sensor.

Scholars at home and abroad have developed systems with different performance parameters [4-7], but the methods are unitary for simulating spectral properties, colour temperature type and the optical performance parameter of magnitude. They often place different band-pass filters in front of the light source to simulate stellar spectrums [8-11]. In addition, different neutral filters are placed behind the light source to simulate different magnitudes [5, 8, 12, 13]. But the filter with any passing or blocking properties can not be made, so the spectrum simulation types are unitary with low precision and poor flexibility. The transmittance coefficients of neutral filters are fixed. Moreover, the filters are not flat enough, and their photic zones are not wide enough. As a result, the accuracy of the magnitude regulation is low, the usable spectral region is narrow, the properties of the simulated spectrums are affected and the flexibility is poor. Thus, the aerospace engineering requirements for star simulator technology cannot be satisfied.

This article introduces a creative new single star simulation system, which achieves multi-colour temperature, wide star magnitude range output and high simulation precision. In addition, the colour temperature and simulation for star magnitude do not interfere with each other and can be adjusted in real time. Experiments are carried out to evaluate the performance of the proposed system.

2. Design of the single star simulator

The system divides the light emitted from the light source into the output light of a number of different spectral bands with adjustable intensity and then mixes them evenly to control the overall intensity of the light output. The overall structure of the system is shown in Fig. 1. The system includes 7 key components: an industrial personal computer, an electric control box, a light source, a band intensity controller, a six-prism integral ball, a magnitude controller and a power source. The light source and the band intensity controller are connected with one inlet and multiple outlet optical fibres (including 2 quartz paths and 11 glass paths), while the band intensity controller and six-prism integral ball are connected with multiple inlets and a one-outlet light fibre (including 2 quartz paths and 11 glass paths).

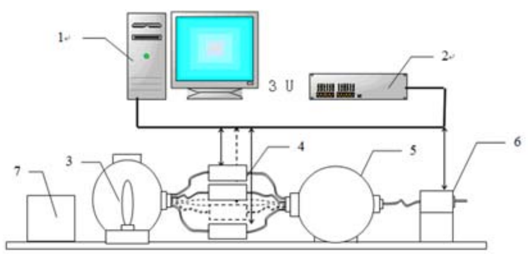

1-IPC; 2-Electric control box; 3-Light source; 4-Band intensity controller; 5- Six-prism integral ball; 6-Magnitude controller; 7-Power source.

Fig. 1. The structure of the new single star simulator.

The working process of the system is as follows. The light emitted from the light source forms multi-beam light rays with different narrowband spectrums and different light intensities after passing through the 13 band intensity controllers. These light rays are then evenly mixed in the six-prism integral rod to realize the simulation of different colour temperatures through controlling the light intensity of each colour light. And thereby to realize the simulation of different magnitudes through controlling the uniform light intensity output using the magnitude simulator. In addition, the IPC, electric control box, light source, band intensity controller, and magnitude controller are connected with an RS-485 bus. In this way, the simulator not only separately controls each part but also controls the overall system.

2.1 Design and Implementation of the light source

The light source of the single star simulator should cover each band of light to the greatest extent possible. Therefore, this study employed a supplemental lighting method using a 150 W xenon lamp and an 850 nm LED light. The spectrogram after light supplementation is shown in Fig. 2.

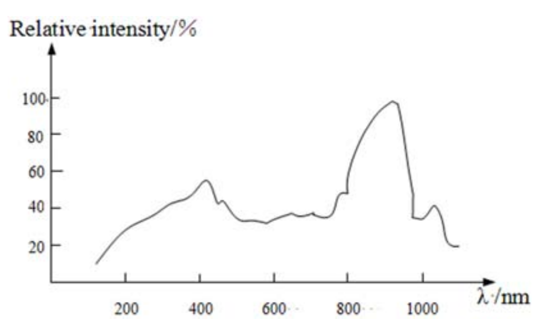

Fig. 2. The spectrogram of the system's light source.

Fig. 2 demonstrates that the spectral range of the peak value of emitted light crosses the infrared, visible and ultraviolet light spectrums, which meets the design requirements of 350 nm to 950 nm.

The light source is composed of a 150 W xenon light, a power source, a controller, a reflector and an optical fibre output coupler.

2.2 Design and implementation of the band intensity controller

To simulate different colour temperatures, the thesis divided the light emitted from the light source into a number of paths through a one-inlet and multiple outlet optical fibre bundles and then separately input the light paths into each light band intensity control unit. In this study, the light was divided with a spectral range from 350 nm to 950 nm into a band every 50 nm, forming 13 paths of narrowband light with a central wavelength of 350 nm, 400 nm…900 nm and 950 nm. The method for producing different central wavelengths will be explained in greater detail below. A light band intensity controller for a total of 13 paths of light was needed.

A large number of sub-light sources with nearly identical structures were to be controlled. Therefore, a modular design was used. That's to say, 13 identical light band intensity control units were used to simplify the system structure and facilitate maintenance. One noteworthy point is that part of the spectral range of the light source reaches the ultraviolet light region. Thus, quartz optical fibres were used instead of glass fibres in two (350 nm and 400 nm) of the 13 optical fibre sub-light paths. Glass optical fibres were used in the other paths.

The structures of each sub-optical path are the same. As shown in Fig. 3, the incident light passes from the optical fibre input coupler to the collimating lens. After beam expansion and collimation, the light passes to the iris diaphragm. It is then filtered by narrowband filters. Light output occurs after passing a 10% reflector.

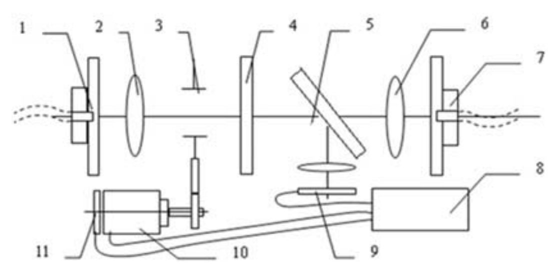

1、7- Optical fiber coupler; 2-Collimating lens; 3- Iris diaphragm; 4-Narrowband filters; 5-10% reflector; 6-Convergent lens; 8- Control panel; 9-Photocell; 10-Stepper motor; 11- Code disk.

Fig. 3. The structure of each band intensity control unit.

2.2.1 Realisation of different light intensities

As shown in Fig. 3, the reflected light passing through the 10% reflector is reference light. The light intensity of each colour light can be measured after passing through a photocell. This light is the input for the control panel. It is then fed back to the stepper motor for adjusting in the iris diaphragm. In this way, real-time management is realized for the light intensity of each colour light. When the system needs to be calibrated, the stepper motor is controlled by a code disk.

2.2.2 Realisation of different central wavelengths

The control of the spectrum is realized through the narrowband filters. According to the design requirements, the central wavelengths of each narrowband filter are 350 nm, 400 nm…900 nm and 950 nm. The incident light is filtered into 13 paths of colour light with different central wavelengths and certain band-widths after passing through these filters.

The 13 paths of colour light comprise the input for the six-prism integral ball through the optical fibre. The light is then mixed evenly through diffuse reflection. The simulation of different colour temperatures of the stellar light sources can be realised by adjusting the light intensity of each light colour.

2.3 Design and implementation of the magnitude controller

After being evenly mixed, the light rays pass into the magnitude controller. The magnitude range that must be simulated is 0 to +6.5 MI. Thus, the maximum light intensity is 398 times (2.518×6.5=398 times) greater than that of the minimum light intensity. Therefore, this research used a mirror attenuation array with an iris diaphragm, as shown in Fig. 4.

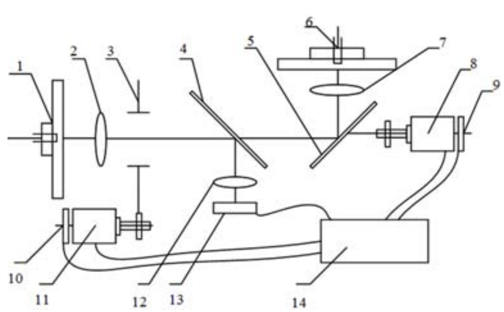

1、6-Optical fiber coupler, 2-Collimating lens; 3-Iris diaphragm; 4-10% reflector, 5- The reflector attenuation array; 7、12-Convergent lens; 8、11-Stepper motor; 9、10-Code disk; 13- Photocell; 14-Control panel.

Fig. 4. The structure of magnitude controller.

As shown in Fig. 4, to complete the large proportional attenuation of the light intensity, the reflector attenuation array must be driven by another stepper motor, while the iris diaphragm must be used to complete the small range adjustment of the light intensity. The reflector attenuation array performs 100%, 10% and 1% attenuations. Thus, it roughly divides the uniform light into three intensity levels, after which the iris diaphragm completes the subdivision at each level.

This research used 10% and 100% reflectors to realise 3 types of attenuation of the uniform light. It was necessary to place reflectors with different combinations, as shown in Fig. 5.

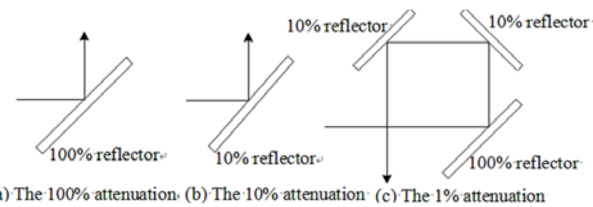

Fig. 5. The 3 kinds of attenuations of the reflector attenuation array.

To simplify the structure and facilitate operation of the device, this work mounted the mirror groups on a fixed base, with the base rotated by the stepper motor. The specific assembly is shown in Fig. 6.

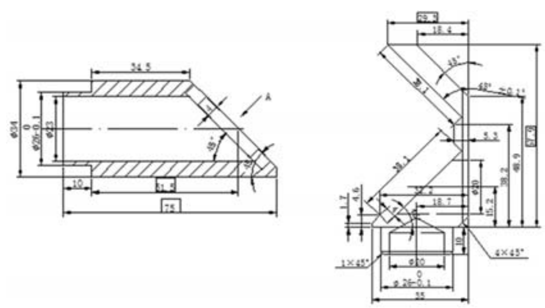

Fig. 6. The assembly diagram of the mirror groups.

Another advantage of the adjustment method is that the reflector is not sensitive to the spectral distribution. Thus it does not influence the spectral simulation results.

3. System testing and discussion

Using the above design, this study installed the system and built a testing platform in the laboratory.

3.1 Colour temperature simulation results

The test instrument was a spectrometer, and the software was OSM-Analyst. The colour temperatures simulated in the laboratory include 2,600 K, 3,600 K, 4,300 K, 5,000 K, 5,500 K, 6,000 K, 6,800 K, 7,600 K and 9,800 K. From these colour temperatures, the research obtains the relevant spectral fitting curves. For instance, the spectral fitting curves for 2,600 K, 5,000 K, 7,600 K and 9,800 K are shown in Fig. 7.

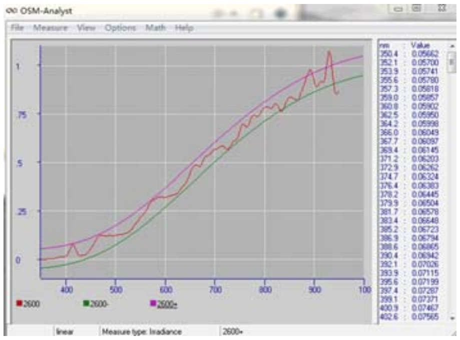

(a) 2600K

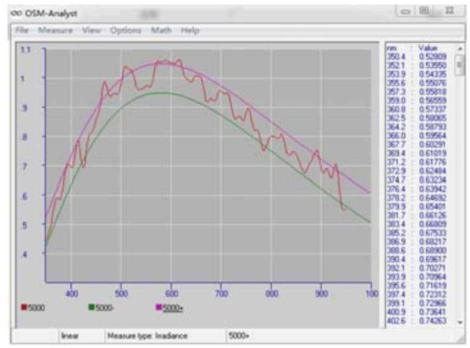

(b) 5000K

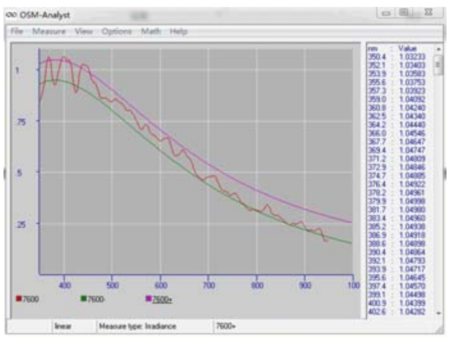

(c) 7600K

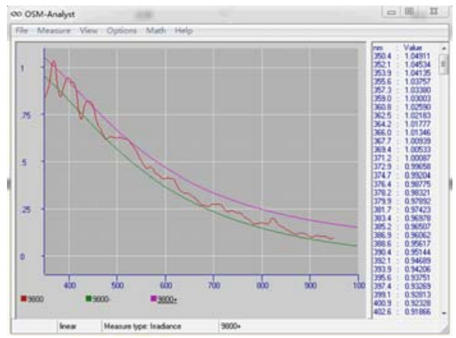

(d) 9800K

Fig. 7. The spectral fitting curves of 2600 K, 5000 K, 7600 K and 9800 K.

In Fig. 7, the red curve represents the fitting curve for the colour temperature. The purple and green curves represent the ±0.1 envelope lines of the corresponding standard colour temperature curve. The Fig. 7 indicates that the fitting curves fall within the regions covered by the envelope lines. Thus, the relative errors of the fitting curve and the standard colour temperature curve is less than or equal to ±0.10.

Thus, the method used in this research can simulate the equivalent colour temperature of a stellar light source because the fitting curve is broadly in line with the standard colour temperature curve and the simulation situation is good.

Table 1. The illumination values measured for each colour temperature.

9800K	7600K	6800K	6000K	5500K	5000K	4300K	3600K	2600K
2.17	2.1	2.09	2.18	2.12	2.15	2.13	2.11	2.05
1.32	1.32	1.31	1.35	1.34	1.34	1.33	1.33	1.30
0.83	0.84	0.81	0.86	0.84	0.85	0.82	0.81	0.82
0.53	0.52	0.51	0.55	0.53	0.54	0.53	0.52	0.52
0.35	0.34	0.32	0.37	0.34	0.35	0.34	0.31	0.32
0.22	0.21	0.24	0.23	0.20	0.20	0.22	0.21	0.20
0.13	0.14	0.13	0.12	0.13	0.14	0.13	0.13	0.12
0.085	0.08	0.086	0.079	0.086	0.088	0.085	0.081	0.084
0.05	0.052	0.054	0.049	0.055	0.051	0.055	0.052	0.055
0.03	0.031	0.035	0.034	0.034	0.029	0.036	0.034	0.035
0.021	0.022	0.02	0.019	0.022	0.023	0.024	0.019	0.02
0.013	0.014	0.015	0.012	0.014	0.011	0.012	0.013	0.012
0.008	0.007	0.006	0.009	0.008	0.009	0.008	0.007	0.008
0.005	0.004	0.005	0.005	0.005	0.006	0.005	0.005	0.005

3.2 Magnitude simulation results

The output light of the system first passed through the 2 m collimating parallel light pipe. Next, a SPD-Ⅲ micro light illumination instrument was used to measure the illumination of the output star point image. The illumination values measured for each colour temperature are shown in Table 1 in unit of ($\times 10^{-6}$ lx).

According to Table 1, the corresponding magnitude can be calculated from the relationship between the magnitude and the illumination [14-15]. Through calculations, the thesis concludes that the magnitude simulation range of the system is between 0 and +6.5 MI and that the relative error between the magnitude simulation and the standard value is less than or equal to ±0.3 MI. From this, this work can be certain that the system can simulate the equivalent magnitude of a stellar light source and that the simulation is large in range with high precision, thereby meeting the design requirements.

4. Conclusions

A new single star simulator was designed in this article to overcome the shortcomings of existing star simulators for conducting spectral and star magnitude simulations. The innovation points are as follows:

(1) The system light source adopted a method for filling light with a xenon lamp and a LED light, which replaced the traditional halogen lamp or LED lamp, thereby greatly increasing the coverage of the light source spectrum.

(2) After separating the light emitted from the wide-spectrum light source, light band intensity control units with different band-pass filters and an electric diaphragm formed several paths of narrow-band colour light with adjustable intensity and different bands, which were then mixed evenly to obtain stellar spectra simulation effects with high precision and great flexibility. This scheme is the first in the history of the industry. It overcomes the deficiencies of existing star simulators that depend only on band-pass filters, such as low precision and poor flexibility for conducting spectral simulations.

(3) This research used a segmented attenuator with a wide spectrum reflectivity composed of a rotatable reflector installation disk to adjust the high intensity light. Stepping adjustment was conducted for low light intensities using an electric iris diaphragm. This enable wide spectrum passing that was insensitive to light intensity adjustment, which allowed obtaining good spectrum distribution and control of magnitude adjustment over a wide dynamic range. This scheme is also the first in the history of the industry. It overcomes the deficiencies of existing star simulators that depend solely on neutral colour filters, such as small adjustment ranges, low precision and narrow usable spectral regions, which affect the simulated spectral properties and leads to poor flexibility when conducting magnitude simulations.

In this study, the performance indexes for the single star simulator spectrum and magnitude simulation designed are excellent.

In conclusion, the primary advantage of this system is that it can achieve multi-colour temperatures and wide-magnitude-range output with high efficiency, precision and flexibility. Based on this study, the instrument has already been used in engineering applications. Up to date, it has been in good working order without any breakdown. This system will be of great significance for scientific research and engineering.

Acknowledgments

The authors would like to acknowledge support from the National Nature Science Foundation of China (No. 50627502), Fundamental Resources Platform of Science and Technology of Sichuan Province in China (No. 10PT-01) and The Supporting Program of Science and Technology of Sichuan Province in China (No. 2012GZ0004).

References

[1] A. Jamshaid, J. C. Fang, Transactions of Nanjing University of Aeronautics & Astronautics, **22**(2), 132 (2005).
[2] F. Duan , J. Y. Liu, F. Yu , Transactions of Nanjing University of Aeronautics & Astronautics, **22**(2), 165 (2005).
[3] E. A. Vitriencho and B. Y. Dolgopolov , Cosmic Research, **31**(4), 3613 (1993).
[4] G. F. Sun, G. Y. Zhang , H. L. Jiang , Y. G. Hao, Y. J. Gao, Optics and Precision Engineering, **19**(8), 1730 (2011).
[5] X. Y. Sun, G. Y. Zhang, D. Y. Wang, Y. C. Hao, J. Duan, Chinese Journal of Scientific Instrument, **32**(9), 2121 (2011).
[6] S. Umamaheswaran, Santosh Nagendra, National Aerospace and Electronics Conference, Proceedings of the IEEE, 139 (2009).
[7] S. E. Kendrick, Christopher Rob, Dennis Ebbets, Paul Atcheson, Proceedings of SPIE - The International Society for Optical Engineering, 6265 (2006).
[8] G. J. Feng, Z. Ma, Y. C. Li, Journal of Applied Optics, **31**(1), 39(2010).
[9] Y. S. Weng, Z. G. Xie, J. H. He, F. Y. Weng, Application of Integrated Circuits, **37**(3), 42 (2011).
[10] W. M. Zhang, X. C. Wang, Yi Ma, H. F. Duan, Opto-Electronic Engineering, (25), 74 (1998).
[11] Y. Chen, W. M. Zhang, Opto-Electronic Engineering, **37**(8), 24 (2010).
[12] Y. P. Liu, J. Li, H. Zhang, Infrared and Laser Engineering, (35), 331 (2006).
[13] C. G. Zhao, J. B. Tan, J. Liu, Y. H. Wang, Optics and Precision Engineering, **18**(6), 1326 (2010).
[14] B. T. Tan, G. Y. Jing, B. G. Wang, Y. C. Yuan, Infrared and Laser Engineering, (35), 397 (2006).
[15] B. T. Tan, C. Y. Jiang, B. G. Wang, X. Zhang, X. W. Guan, High Power Laser and Particle Beams, **21**(2), 221 (2009).

*Corresponding author: nic6700@scu.edu.cn